IEEE Access
Multidisciplinary | Rapid Review | Open Access Journal

Received November 20, 2019, accepted December 23, 2019, date of publication December 31, 2019,
date of current version January 10, 2020.

Digital Object Identifier 10.1109/ACCESS.2019.2963225

Circuit Level Modeling of Electrically Doped Adenine–Thymine Nanotube Based Field Effect Transistor

DEBARATI DEY[1,2], DEBASHIS DE[2,3], (Senior Member, IEEE), FERIAL GHAEMI[4], ALI AHMADIAN[5], AND LUQMAN CHUAH ABDULLAH[4]

[1]Department of Electronics and Communication Engineering, B. P. Poddar Institute of Management and Technology, Kolkata 700052, India
[2]Department of Computer Science and Engineering, Maulana Abul Kalam Azad University of Technology, Kolkata 741249, India
[3]Department of Physics, The University of Western Australia, Perth, WA 6009, Australia
[4]Institute for Tropical Forestry and Forest Products, Universiti Putra Malaysia (UPM), Serdang 43400, Malaysia
[5]Institute for Mathematical Research, Universiti Putra Malaysia (UPM), Serdang 43400, Malaysia

Corresponding authors: Debarati Dey (debaratidey@yahoo.com) and Ali Ahmadian (ahmadian.hosseini@gmail.com)

This research was financially supported under 1. University Grants Commission, India for the project under UGC Major Project File No.: 41-631/2012 (SR). 2. FRGS grants (Grant No.: 01- 01-18-2031FR) and (Grant No.: 03-01-19-2193FR) provided by the Ministry of Education, Malaysia and Universiti Putra Malaysia.

ABSTRACT We investigate the gate-controlled, electrically doped tunnelling current in Adenine-Thymine heterojunction nanotube-based Field Effect Transistor (FET). This analytical model FET is designed by Density Functional Theory (DFT) and Non-Equilibrium Green's Function (NEGF) based First principle formalisms. It is demonstrated that Band to Band Tunnelling (BTBT) is possible in relaxed Adenine-Thymine heterostructure nanotube. The evaluation of BTBT tunnelling probability to estimate tunnelling current for only ± 0.01V applied bias voltage is calculated using Wentzel-Kramers-Brillouin approximation. Electrical doping is introduced to eliminate the probability of fault generation. By keen observation on the shift of energy levels in the band structure, the availability of high transmission co-efficient peaks and current-voltage response we demonstrate the Schottky barrier nature for this geometrically pre-optimized bio-molecular FET. The doping concentration is varied from 0.0001V to 0.1V to achieve a substantially large amount of tunnelling current when the electronic temperature is kept at 300K. The E-k diagram or complex band structure of this heterostructure nanotube ensures its in-direct semi-conducting nature. This is a first attempt to present a circuit-level demonstration using this Adenine-Thymine nanotube-based bio-molecular FET and validate the obtained results with the existing approaches.

INDEX TERMS Adenine-thymine, DFT, nanotube, NEGF, TFET.

I. INTRODUCTION

The tunnel FET (TFET) has been proved as a strong candidate for future generation low power application due to its low sub-threshold slope. Though Silicon does not achieve low sub-threshold slope and sufficiently high ''ON''-state current due to its indirect energy bandgap, therefore alternative channel materials for FET are being investigated [1], [2]. In the field of organic electronics, recently Carbon Nano Tube (CNT), Graphene nano-ribbon based FETs draw the attraction of the researchers [1], [3]–[5]. Due to high carrier mobility and zero-band gap, graphene nano-ribbon FET fails to prove itself in the field of transistor application [1], [6]. Researchers are also trying to find an alternative TFET due to the presence of leakage current in the MOSFET which uses SiO_2 as gate dielectric [7], [8].

In this study, BTBT probability through the bio-molecular channel has been investigated using DFT conjugated with NEGF based First principle approach with the help of Atomistix Tool Kit-Virtual Nano Laboratory (ATK-VNL) software simulator package version 12.8.0. Considering Poisson's solution the drain current of this bio-molecular TFET is being investigated at 300K electronic temperature. To avoid the probability of fault arising, electrical doping is introduced to design the analytical model TFET. In case of electrical doping, a potential drop is to be created between the two terminals of a system or in this case the two terminals of electrodes by inducing two different and opposite potentials

The associate editor coordinating the review of this manuscript and approving it for publication was Atif Iqbal.

TABLE 1. Comparative study of existing FETs and proposed bio-molecular FET.

FETs / Features	EXISTING TFET				Proposed TFET
	CNT hetero-junction TFET [3]	Graphene nanoribbon FET [5]	Si-MIS FET [9]	SOI MOSFET [10]	Adenine-Thymine hetero-junction bio-molecular TFET
Based on	DFT+EHT	DFT	Real space Green's function	First principle Ab-initio	DFT+NEGF
Composites	CNT	Zigzag Graphene nanoribbon	Silicon	Silicon	Adenine-Thymine nanotube
Applied Bias (V)	-0.2 to +0.6	0 to 0.4	-10 to +15	0.2 to 1.2	±0.001 to ±0.1
Electron Temperature	–	–	–	<50K	300K
Stress (eV/A^3)	–	–	–	–	0.01
Force tolerance (eV/Å)	0.05	0.05	–	–	0.01
Operating frequency	–	–	–	–	25 THz

at the two ends of the electrodes. The difference between the two potentials leads to movement of charge from one terminal to another through the central molecular region. Even more, the amount of electrical doping can be calculated using the length, width, height and the amount of charge which is applied at the two terminals of the molecular device. On the contrary, normal doping is the process to incorporate dopants (either n-type or p-type impurity) into the materials by ionization technique or by ion bombarding method. This process is a high-temperature process. This process leads to some fault generation within the materials as it is a high heat process.

The comparison Table 1 show a comparative study between the existing FET's and the proposed Adenine-Thymine nanotube-based TFET.

The major contributions of this work are listed as follows:

1. An approach to design an analytical model of Adenine-Thymine based heterojunction bio-molecular nanotube-based TFET.
2. Sufficiently large current obtained and the Current-Voltage (I-V) response follows almost the same characteristics of conventional FET.
3. This is an approach to analytically design molecular level circuit (mainly logic devices) and validate the result with the result obtained from the multi-sim software simulator.

II. COMPUTATIONAL METHOD

The quantum-ballistic BTBT is observed for the theoretical model of Adenine-Thymine based nanotube TFET. This bio-molecular TFET is designed using $1\times1\times100$ K-point samplings and 75 Hartree mesh cut-off energy.

The molecular device has extremely small dimensions for width (X-direction) and height (Y-direction) compared to its' length. The length is considered to be projected along Z-direction. To minimize error-free calculation, the number of K-point sampling has been increased along the length or Z-direction. Increasing the no. of samples along Z-direction, we increase the no. of samples along the central scattering region of the molecules and therefore, the more accurate and

TABLE 2. Computational parameters.

Parameter	Value
Configuration	(x, y, z)
Fermi Level	0 eV
Poisson Solver	FFT2D
Input Voltage	0V-±0.02V
Basis set	Hoffmann
Device Algorithm	Krylov
Close neighbour distance	0.02 nm
Maximum no. of Steps	150
Step size	0.2 nm
K-points	1×1×100
Generic weighting Scheme	Wolfsberg
Exchange correlation function	Local Density Approximation-Generalized Gradual Approximation (LDA-GGA)
Hybridization	Mono/ Single hybridization
Hückel Basis set	Hoffmann
Time period	1 fs
Energy	3.02 eV

significant result has been obtained. Density Functional Theory (DFT) calculations and LDA-GGA functional are used in this manuscript. DFT reduces the quantum mechanical ground state many-electron problem to self-consistent one-electron form, through the Kohn-Sham equations. To calculate the quantum-mechanical transport phenomenon DFT is used in this calculation. This technique is also a good balance between computational cost and accuracy. This method also describes the exchange-correlation functional of the molecules. Moreover, DFT is, in principle, more accurate explicitly correlated quantum chemistry method to describe the function of the molecular devices.

LDA-GGA method is the local density approximation-generalized gradient approximation method. This method provides a possible explanation for the predicted low diffusion coefficients for the simulations of the molecular device and raises a general concern over the ability of pure functional to describe the intra-molecular deformation and also highlighting the importance of exact exchange in simulations

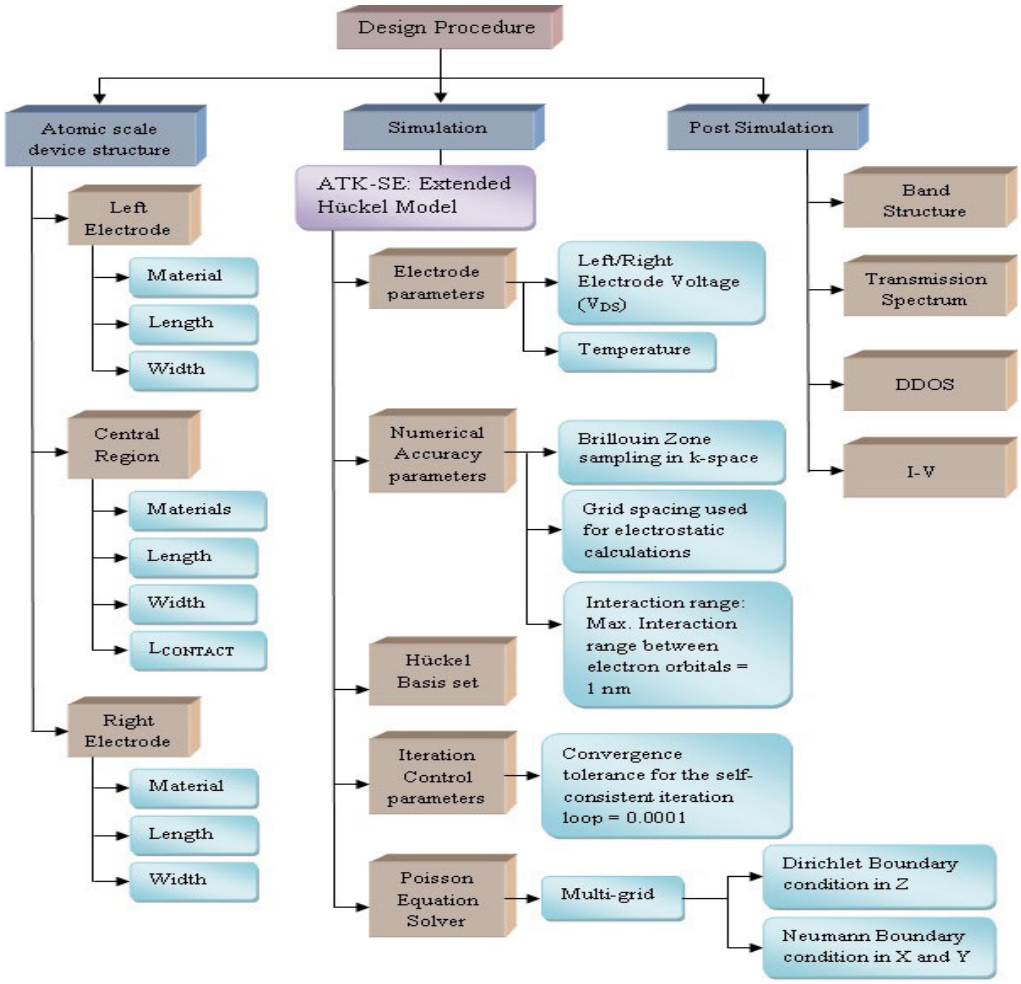

FIGURE 1. Flow diagram of the ATK-VNL software simulator.

of at molecular level. More specifically LDA shows in terms of the electron density at that point. This also means that the exchange-correlation functional which was recorded as an integral of a certain function of spatial variables of the central molecular region of the device.

DFT process is officially exact, but for realistic calculations, the exchange-correlation energy as a functional of the density must be approximated. For this reason, LDA is a standard choice. Simple LDA results in a realistic description of the atomic structure, elastic, and vibration properties for broad varieties of systems. Yet, LDA is generally not so accurate to describe the energy of chemical reactions (for example, heats of reaction and activation energy barriers), leading to an over the rate of the binding energies of molecules and solids in particular. Recently, GGA's have overcome such deficiencies to a considerable extent, giving, for instance, a more realistic description of energy barriers in the dissociative adsorption of hydrogen on metal and semiconductor surfaces. Gradient corrected or GGA functions depend on the local density as well as on the spatial variation of the density.

The maximum tolerance parameter is 10^{-5} along with 200 steps of operation. The simulation parameters are required for this theoretical modelling of nano FET, shown in Table 2.

The working principle and work-flow model of Quantumwise software are illustrated in Fig.1.

III. RESULTS AND DISCUSSION

This work presents an analytical approach to design Adenine and Thymine bio-molecule based heterojunction nanotube TFET using First principle formalisms. Therefore, at first, we take two 4×4 nanolayers of Adenine and Thymine bio-molecules. After the necessary simulation arrangements, this heterostructure nanotube has been analytically designed. Henceforth, the nanotube is aligned properly and also geometrically optimized to reduce the stress at a molecular level. The nanotube is 2.44nm long and 0.83nm wide. This molecular device is divided into three main portions, viz; left electrode (LE), right electrode (RE) and central molecular region, which are mentioned in Fig. 2. Additional metallic gate with a small di-electric layer is placed at the top of this bio-molecular nanotube to form the TFET. The LE and RE are 0.5nm long. This two probe experiment is carried out using ATK-VNL software simulator package of version 12.8.0.

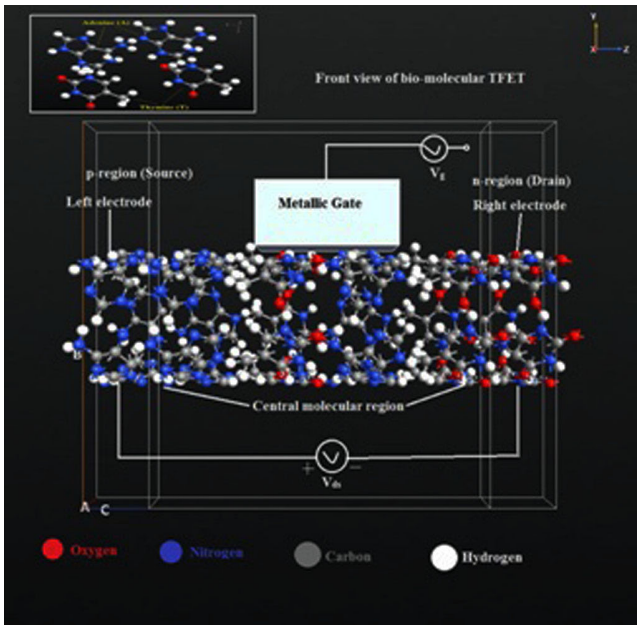

FIGURE 2. Atomistix model of bio-molecular nanotube TFET.

This atomistix bio-molecular TFET shows almost ideal characteristics like conventional FET. Adenine and Thymine are two crucial molecules of the human body which form the DNA chain. Adenine converts itself into adenosine-tri-phosphate (ATP) and takes an active part in human metabolism. Adenine and Thymine chain based electrically doped p-i-n FET is already reported [11]. The various quantum-electronic characteristics of this bio-molecular nanotube-based TFET have been observed such as:

1. Transmission spectra.
2. Device Density of States.
3. I-V characteristics.
4. Conductance
5. Circuit level implementation and its validation.

This nanoscale bio-molecular TFET is designed considering electrical doping procedure to form p and n regions at the two ends of the nanotube. The structural information of the bio-molecular TFET is observed in Table 3.

The procedure of electron contribution and electron acceptation to the molecular thin films is described as electrical doping. Introducing this procedure molecular interface can be modified [11]–[13]. There are several advantages of electrical doping, some of them are increased device efficiency when injecting carrier at the molecular interfaces and molecular film conductivity increased to a great extent, Ohmic contact can be achieved on inorganic semiconductor without using conventional dopants etc. [11], [14], [15]. The doping concentration is calculated using the following calculation in Eq. (1)

Effective doping concentration=doping/volume [11], [16]

In this work, the electrical doping charge is varied from ±0.001V to ±0.1V. Assume Effective doping charge= ±0.1V.

TABLE 3. Structural information of p and n bio-molecular TFET.

Bio-nanotube TFET structural specification	n-type bio TFET	p-type bio TFET
Channel length	2.45 nm	2.45 nm
Gate length	1 nm	1 nm
Nanotube diameter	3.84 nm	3.84 nm
Nanotube length	1.72 nm	1.72 nm
Source doping	5.45×10^{18} (n-doping)	5.45×10^{18} (p-doping)
Drain doping	5.45×10^{18} (n-doping)	5.45×10^{18} (p-doping)
Gate di-electric thickness	0.1 nm	0.1 nm
Aspect ratio	2.2	2.2
Transconductance gm	4.62×10^{4} S	3.39×10^{3} S
Drain resistance I_d	$4.9\times10^{-5}\Omega$	$1.53\times10^{-3}\Omega$
Amplification factor μ	2.27	5.17

TABLE 4. Doping concentration w.r.t. Applied electrical charge.

Electrical Charge (V)	Doping concentration (per cc)
±0.001	5.45×10^{17}
±0.01	5.45×10^{18}
±0.1	5.45×10^{19}

Volume of the nanotube=length × width × height = $(2.44\times10^{-7})\times(0.83\times10^{-7})\times(0.9\times10^{-7})\text{cm}^{-3} = 1.822\times10^{-21}$

$$\text{Hence, Effective doping} = \frac{0.1}{1.822\times10^{-21}} = 5.45\times10^{19}/\text{cm}^3 \quad (1)$$

Doping concentrations obtained for various potentials are listed in Table 4.

A. TRANSMISSION SPECTRA

Transmission spectra are the amount of electromagnetic radiation which can pass through t inter atomic passage. The sharp and wide peak of transmission assures the availability of the channels within the central molecular region.

It is also observed that, if the number of available peaks is increased within the bias window that means large numbers of channels are available. Therefore, the high tunnelling current can flow through the central molecular region. Bias window simply depends on the amount of electrical doping charge. If the doping concentration is high then the transmission is also high. The compared transmission spectra are shown in Fig. 3, where 'green' colour represents transmission spectra when doping charge is ±0.001V and 'red' line shows transmission spectra for ±0.01V doping charge. Hence transmission co-efficient simply depends on the applied bias and the energy levels, that can be formulated using Green's function in Eq. (2)

$$T(E, V_d) = T_r\left(\Gamma_1 G^R \Gamma_r G^A\right) \quad (2)$$

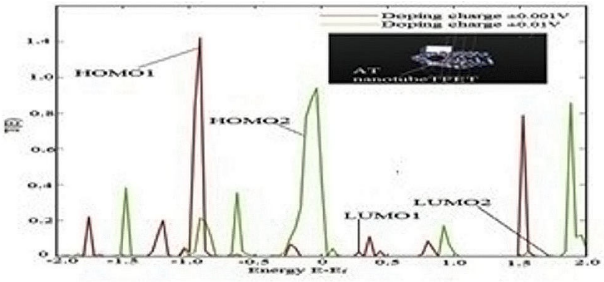

FIGURE 3. Compared transmission spectra of bio-molecular nanotube TFET.

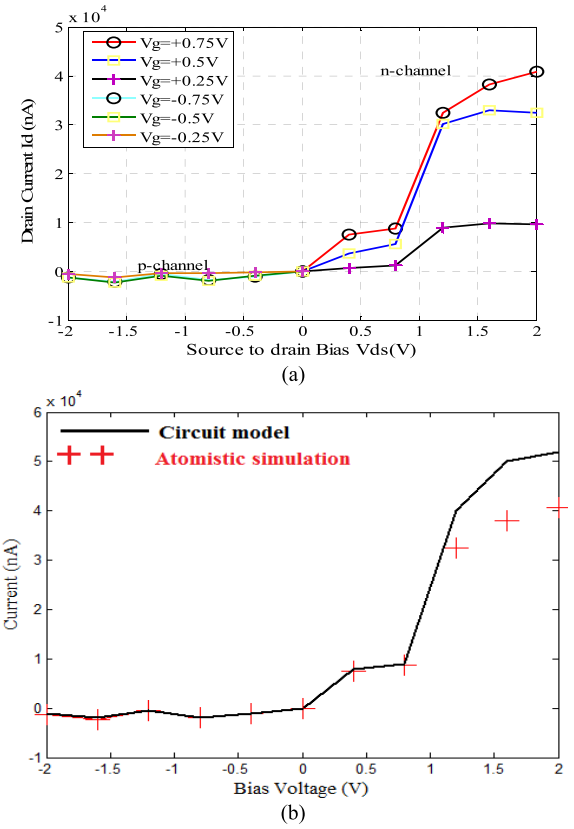

FIGURE 4. (a) I_d –V_{ds} graph of bio-molecular nanotube TFET. (b) Multi-sim simulated I-V graph of the circuit model representation for FET (solid line) and the atomistic simulated data (plus symbols) of the same device, when V_g is constant.

where bias dependent transmission co-efficient is expressed as $T(E, V_d)$, the impeded and complex Green's function of the fundamental bio-molecular scattering segment is articulated as $G^{R/A}$ [17]. Highest Occupied Molecular Orbital (HOMO) and Lowest Unoccupied Molecular Orbital (LUMO) for the two doping conditions are shown in Fig. 3. HOMO and LUMO are referred to as the maxima of the valence band and the minima of the conduction band respectively. The difference between HOMO and LUMO signifies the thermo-dynamic stability of the molecule. It is also signified that if the gap between these two is maximum then the potential barrier is high which results in less amount of carrier transmission. Minimum gap between HOMO and LUMO means small potential barrier thus it contributes towards high carrier transmission.

B. I-V CHARACTERISTICS

The Current-Voltage (I-V) response of this hetero-structure nanotube supported Adenine-Thymine TFET is shown in Fig. 4 (a). The I-V characteristics which are revealed in Fig. 4 (a), is the result of quantum-ballistic transmission carrier within the central molecular region. This characteristic depends on the electrical doping concentration. When the doping concentration increases then the amount of current transmission also increases. From Fig. 4(a) it is evident that large current is obtained for n-channel whereas very less amount of current has been observed for p-channel.

The contact potential at p and n region has been dropped due to electrical doping. The electrons near the orbital of the Fermi level (E_f) are de-localized and also accountable for this current transportation phenomenon within the central molecular region. If conduction band (E_c) is very close to the E_f than valence band (E_v) then the main donors are received from LUMO. At enough bias voltage E_c shifts in the direction of E_f, and thus energy gap moves near lesser energy height. Therefore, at this bias additional conducting channels contributes to the carrier transportation [18]. This bias voltage is known as the threshold voltage of this TFET. The quantum-ballistic current is formulated in Eq. (3) [11]. The compared I-V characteristics for this device at circuit level modelling and for atomistic simulation, when the gate bias is constant, which is shown in Fig. 4 (b).

$$I_d = \frac{2e^2}{\hbar}\int_{-\alpha}^{+\alpha} T\,(E,V_d)\,[f_L\,(E-\mu_L) - f_R\,(E-\mu_R)] \quad (3)$$

In Eq. (3), I_d is dependent on $T(E,V_d)$ which is bias dependent (here doping charge-dependent) transmission co-efficient, $f_{L/R}$ is the Fermi levels for left and right electrodes, $\mu_{L/R}$ is the chemical potentials of the left and right electrodes. It is observed from Eq. (3), that the drain current I_d is dependent on transmission co-efficient. As a result, for the availability of high transmission peaks which are responsible for higher current is obtained. Above threshold bias voltage more transmission peaks are available due to the availability of more energy states. Therefore, a higher current is obtained above threshold voltage [19], [20].

The drain current (I_d) vs Source to drain bias (V_{ds}) for different gate bias is shown in Fig. 4(a). The I_d-V_g graph for this TFET is also shown in Fig. 5 (a). These two graphs show that this bio-molecular TFET shows almost the same I-V characteristics like conventional FET.

The compared I-V characteristics for this device at circuit level modelling and for atomistic simulation, when V_{ds} is constant, which is shown in Fig. 5 (a). The compared graph of

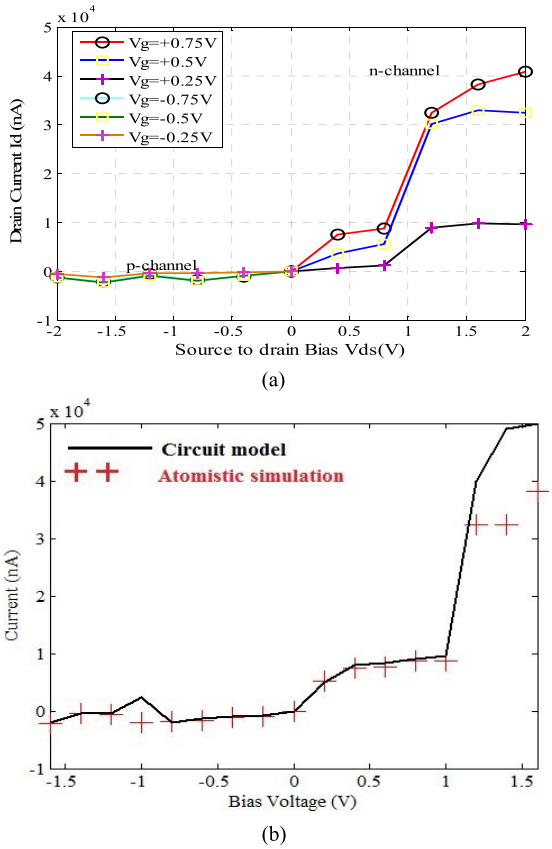

FIGURE 5. (a) I_d –V_g graph of bio-molecular nanotube TFET. (b) Multi-sim simulated I-V graph of the circuit model representation for FET (solid line) and the atomistic simulated data (plus symbols) of the same device when V_{ds} is constant.

this device at circuit level modelling and atomistic simulation is shown in Fig. 5 (b).

C. CONDUCTANCE

The quantum-ballistic transmission property of the device determines channel conductivity of this bio-molecular TFET. This is another important parameter which determines device performance. Channel conductivity depends on the available number of channels present within the transmission bias window.

If this number is higher that means due to the availability of large numbers of channels device conductivity is high. These available channels are responsible for carrier transmission. It is evident from Eq. (3), that I_d is dependent onto the channel's transmission co-efficient. Hence, for the presence of a large number of channels within the bias window increase the channel conductivity [20].

Increasing values of electrical doping concentration increase carrier transmission probability, which is responsible for the high conductivity of the molecular channel. This electrical doping is actually the functional bias at the two terminals of the electrodes, which is also indicated as a source to drain bias V_{ds}. This applied bias is responsible to introduce

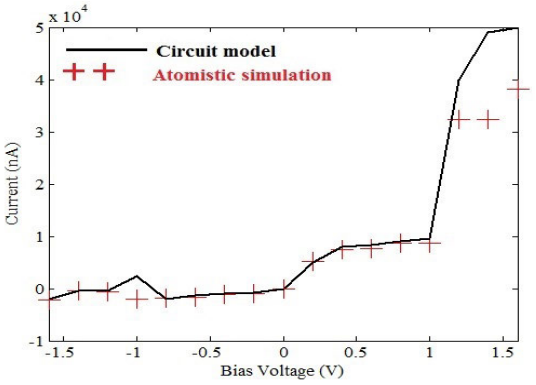

FIGURE 6. Thermal conductivity at different energy levels at different gate bias voltage of bio-molecular nanotube TFET.

TABLE 5. Electronic and structural properties of bio-nanotube based FET's.

FET's	H-C Bond length (Å)	C-N Bond length (Å)	Formation energy (eV/Å)	HOMO (eV)	LUMO (eV)	Electronic nature
p-FET	1.09	1.02	0.41	-1.5	1.94	Semi-metallic
n-FET	1.09	1.02	0.41	-1	0.73	Metallic

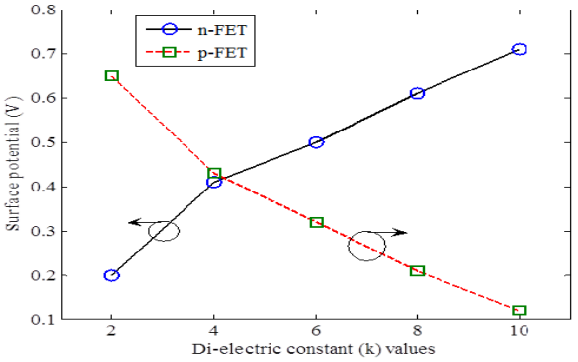

FIGURE 7. Variation in surface potential for different di-electric constants of bio-molecular nanotube TFET.

a potential drop which proceeds as strong potential for introducing conductivity within the channel. When doping density grows, it amplifies the bias; therefore channel conductivity is getting enhanced. The thermal conductivity which is shown in Fig. 6 mainly occurs for electron transmission.

The conductivity of this molecular device is formulated using the Landauer Büttiker formula which is indicated in Eq. (4), where G is the conductivity of the molecular channel, $T(E,V_{ds})$ is the bias dependent transmission co-efficient, f is the average Fermi level.

$$G = \int_{-\infty}^{+\infty} dET\,(E, V_{ds})\,(-\frac{df}{dt}) \tag{4}$$

The differences in structural and electronic properties of these p and n FET are shown in Table 5. The surface potential V_s

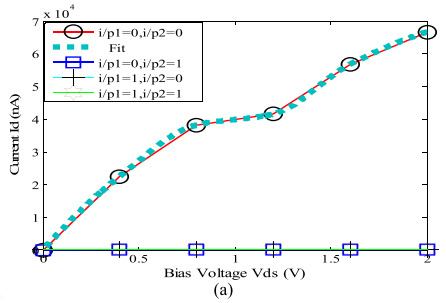

(a)

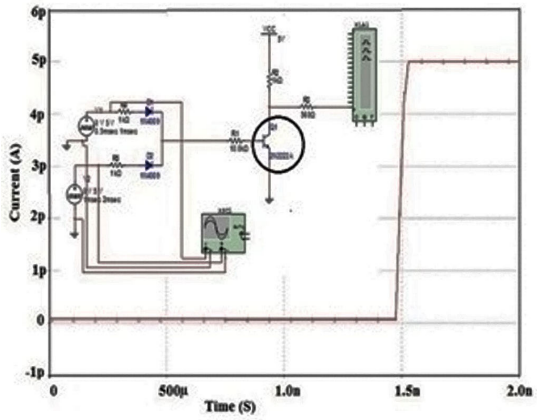

(b)

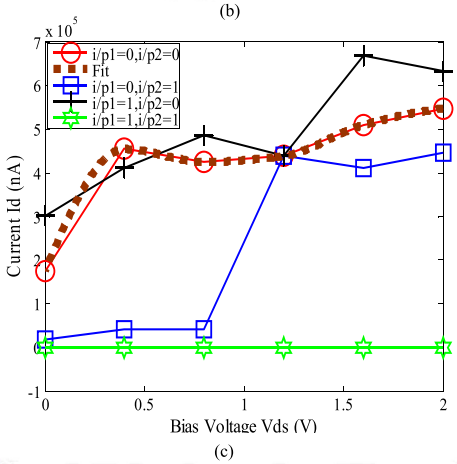

(c)

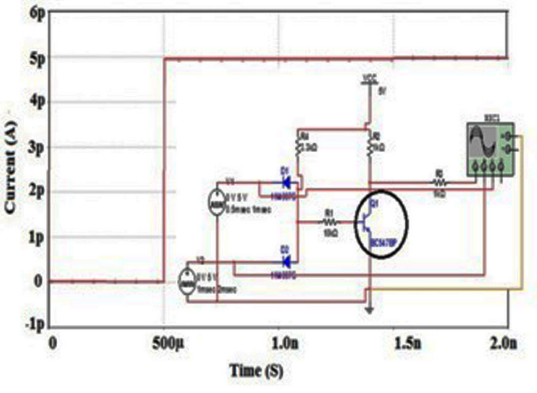

(d)

FIGURE 8. (a) I-V response of the TFET at different bias voltage for the implementation of NOR logic gate. (b) Validation of the result with Multi-sim simulator results for NOR logic gate. (c) I-V response of the TFET at different bias voltage for the implementation of NAND logic gate. (d) Validation of the result with Multi-sim simulator results for NAND logic gate.

TABLE 6. Cross-tick table for statistical comparison between existing TFETs with proposed TFET.

FETs / Features	Existing TFET			Proposed TFET
	CNT FET [3]	GNR FET [4]	Bi-layer GNR FET [5]	A-T hetero-junction TFET
Extremely low bias voltage	√	√	√	√
Room temperature operation	×	×	×	√
Ultra high operating frequency	×	√	×	√
Minimum atomic level stress	×	×	×	√
Significantly large current	√	×	√	√
Optimum force	√	×	√	√

di-electric constant for two types of FET (p and n channel) is shown in Fig. 7.

D. CIRCUIT LEVEL IMPLEMENTATION AND ITS VALIDATION

It is obvious that adjacent atoms attract shared electrons which are present in a covalent bond with the highest electro-negativity. It is a known fact in electromagnetism; positive electrostatic potential attracts negative charge and vice-versa. It is implied that an atom which achieves an affirmative electrostatic potential V_p and the adjacent atom will not be influenced til V_p exceed a given threshold bias V_{th}. When V_p equal to or go beyond V_{th}, then only current flow through the tiny molecular channel. V_p-V_{th} is actually the potential at which exactly no current is available. This V_{th} value depends on the polarity of the bond. Gate bias plays an important role in case of activation of the molecular device. When an applied bias voltage is greater than V_p-V_{th} then only current flows and the device gets activated. This V_{th} depends on the applied potential bias at the gate during the nanoscale simulation process of this A-T based TFET.

The threshold voltage level is used to vary the concentration of electrical doping, which leads to moving the Fermi height of left and right electrodes. Electrical doping concentration is to be changed by changing the potential bias at the two electrodes. Fig. 8 (a)-(d) shows the output observed for the two universal gates NOR and NAND, using this TFET which is originated from Adenine-Thymine nanotube structure and then the results are validated with the graphs obtained from Multi-sim 11.1 [20].

As per the circuit level representation when the applied drain to source bias (V_{ds}) voltage exceeds the V_p-V_{th} value, then current transmits in forward bias. In reverse bias, applied voltage (V_{ds}) is slightly more than V_p-V_{th} and therefore almost no current transmits excluding insignificant leakage

current. So the condition for current flows is shown in Eq. (5).

$$V_{ds} \geq V_{th,l} + 2V_{th} \tag{5}$$

In Eq. (5), $V_{th,l}$ is the modified threshold voltage which has been set for connecting atoms. If V_{ds} is not same or even exceed $V_{th,l}+2V_{th}$, then movement of the current in reverse bias is not possible. The I-V response graph of the circuit level execution of the device and result obtained during the nanoscale simulation is shown in Fig. 5(a). Two universal logic gates NAND and NOR are satisfactorily implemented using atomistix simulation [19], [20].

The statistical comparative study of the various features of the proposed TFET along with the existing FET's is illustrated in Table 6.

IV. CONCLUSION

A detailed analytical model of Adenine-Thymine heterojunction nanotube-based TFET is represented and its' quantum-ballistic transmission is investigated. The I-V response for various applied bias and (at various electrical doping) has been illustrated. Significantly, 61μA current is achieved at 2V applied bias during room-temperature operation. It has been observed that the conductivity of the channel increases due to electronic transmission and increasing electrical doping concentration. This simulated work is carried out at 1000THz frequency. The I-V response of this TFET at different bias helps to implement NAND and NOR logic gates. The results are therefore validated with the existing approach. We expect that this bio-inspired TFET increase the possibility of the future generation circuit-level execution using molecular devices.

REFERENCES

[1] R. K. Ghosh and S. Mahapatra, "Proposal for Graphene–Boron nitride heterobilayer-based tunnel FET," *IEEE Trans. Nanotechnol.*, vol. 12, no. 5, pp. 665–667, Sep. 2013.

[2] A. Schenk, "Rigorous theory and simplified model of the band-to-band tunneling in silicon," *Solid-State Electron.*, vol. 36, no. 1, pp. 19–34, Jan. 1993.

[3] L. Leem, A. Srivastava, S. Li, B. Magyari-Kope, G. Iannaccone, J. S. Harris, and G. Fiori, "Multi-scale simulation of partially unzipped CNT hetero-junction tunneling field effect transistor," in *IEDM Tech. Dig.*, Dec. 2010. pp. 32.5.1–32.5.4. [Online]. Available: https://ieeexplore.ieee.org/abstract/document/5703465

[4] S. K. Gupta and G. N. Jaiswal, "Study of nitrogen terminated doped zigzag GNR FET exhibiting negative differential resistance," *Superlattices Microstruct.*, vol. 86, pp. 355–362, Oct. 2015.

[5] K.-T. Lam and G. Liang, "Computational study on the performance comparison of monolayer and bilayer zigzag graphene nanoribbon FETs," in *Proc. 13th Int. Workshop Comput. Electron.*, May 2009, pp. 1–4. [Online]. Available: https://ieeexplore.ieee.org/abstract/document/5091098

[6] Y. Zhang, T.-T. Tang, C. Girit, Z. Hao, M. C. Martin, A. Zettl, M. F. Crommie, Y. R. Shen, and F. Wang, "Direct observation of a widely tunable bandgap in bilayer graphene," *Nature*, vol. 459, no. 7248, pp. 820–823, Jun. 2009.

[7] E. Nadimi, R. Öcttking, P. Plänitz, M. Schreiber, and C. Radehaus, "First-principles investigation of the leakage current through strained SiO_2 gate dielectrics in MOSFETs," in *Proc. IEEE Semiconductor Conf. Dresden (SCD)*, Sep. 2011, pp. 1–4. [Online]. Available: https://ieeexplore.ieee.org/abstract/document/6068768

[8] E. Nadimi, P. Planitz, R. Ottking, K. Wieczorek, and C. Radehaus, "First principle calculation of the leakage current through SiO_2 and SiO_xN_y gate dielectrics in MOSFETs," *IEEE Trans. Electron Devices*, vol. 57, no. 3, pp. 690–695, Mar. 2010.

[9] L.-N. Zhao, X.-F. Wang, Z.-H. Yao, Z.-F. Hou, M. Yee, X. Zhou, S.-H. Lin, and T.-S. Lee, "Atomistic modeling of the electrostatic and transport properties of a simplified nanoscale field effect transistor," *J. Comput. Electron.*, vol. 7, no. 4, pp. 500–508, Dec. 2008.

[10] M. Tabe, D. Moraru, E. Hamid, A. Samanta, L. T. Anh, T. Mizuno, and H. Mizuta, "(Invited) dopant-atom-based tunnel SOI–MOSFETs," *ECS Trans.*, vol. 58, no. 9, pp. 89–95, Aug. 2013.

[11] D. Dey, D. De, and P. Roy, "Electronic characterisation of atomistic modelling based electrically doped nano bio p-i-n FET," *IET Comput. Digit. Techn.*, vol. 10, no. 5, pp. 273–285, Sep. 2016.

[12] W. Gao and A. Kahn, "Electrical doping: The impact on interfaces of π-conjugated molecular films," *J. Phys., Condens. Matter*, vol. 15, no. 38, pp. S2757–S2770, Oct. 2003.

[13] S. L. Rudaz, "Maximizing electrical doping while reducing material cracking in III-V nitride semiconductor devices," U.S. Patent 5 729 029 A, Mar. 17 1998.

[14] A. Kahn, N. Koch, and W. Gao, "Electronic structure and electrical properties of interfaces between metals and π-conjugated molecular films," *J. Polym. Sci. B, Polym. Phys.*, vol. 41, no. 21, pp. 2529–2548, Nov. 2003.

[15] S. Yu, J. Frisch, A. Opitz, E. Cohen, M. Bendikov, N. Koch, and I. Salzmann, "Effect of molecular electrical doping on polyfuran based photovoltaic cells," *Appl. Phys. Lett.*, vol. 106, no. 20, May 2015, Art. no. 203301.

[16] (2013). *Silicon Nanowires: Tutorial, Version 12.8. QuantumWise A/S. Atomistix ToolKit (ATK), QuantumWise Simulator*. [Online]. Available: http://www.quantumwise.com

[17] Y.-C. Ling, F. Ning, Y.-H. Zhou, and K.-Q. Chen, "Rectifying behavior and negative differential resistance in triangular graphene p–n junctions induced by vertex B–N mixture doping," *Organic Electron.*, vol. 19, pp. 92–97, Apr. 2015.

[18] P. Bai, K. T. Lam, E. Li, and K. K.-F. Chang, "A comprehensive atomic study of carbon nanotube Schottky diode using first principles approach," in *IEDM Tech. Dig.*, Dec. 2007, pp. 749–752. [Online]. Available: https://ieeexplore.ieee.org/abstract/document/4419055

[19] A. Mahmoud and P. Lugli, "Toward circuit modeling of molecular devices," *IEEE Trans. Nanotechnol.*, vol. 13, no. 3, pp. 510–516, May 2014.

[20] D. Dey and D. De, "A first principle approach toward circuit level modeling of electrically doped gated diode from single wall thymine nanotube-like structure," *Microsyst. Technol.*, vol. 24, no. 7, pp. 3107–3121, Jul. 2018.

DEBARATI DEY received the master's degree in technology (M.Tech. in VLSI design) from the University of Calcutta, in 2011. She worked in several organizations, such as Onida, Bengal College of Engineering and Technology. She is currently an Assistant Professor with the Department of Electronics Communication and Engineering, B. P. Poddar Institute of Management and Technology, Kolkata. She is the author of the book chapter published by NOVA, USA. Her research interests are in nano technology, quantum cellular automata, and bio-inspired computing.

DEBASHIS DE (Senior Member, IEEE) is currently a Professor with the Department of Computer Science and Engineering, Maulana Abul Kalam Azad University of Technology (formerly known as West Bengal University of Technology), Kolkata. He is also an Adjunct Research Fellow of The University of Western Australia, Perth, Australia. His research area includes location and power management in mobile network and mobile cloud computing. He received Young Scientist award both in 2005 at New Delhi and in 2011 at Istanbul by International Union of Radio Science, Belgium.

FERIAL GHAEMI received the Ph.D. degree in nanotechnology from the Institute for Advanced Technology, Universiti Putra Malaysia, in 2015. She joined the Institute for Tropical Forestry and Forest Products, in 2016, where she is currently a Postdoctoral Research Fellow. She published more than 30 research works in prestigious CIJ journals. Her main research interests are on synthesis of different types of nanomaterials with applications arising in drug delivery, polymer composites, and microextraction techniques.

ALI AHMADIAN received the Ph.D. degree in applied mathematics from the Universiti Putra Malaysia, Serdang, Selangor, Malaysia, in 2013. He is currently a Fellow Researcher with Universiti Putra Malaysia. He has published more than 60 peer-reviewed scientific publications. He is a Reviewer for 60 international journals. He was involved in several national and international projects related to the applications of fuzzy systems in the real-world systems. His current research interests include fuzzy fractional calculus, interval-valued functions and spectral methods for the solution of fuzzy differential equations, and fuzzy mathematical modeling.

LUQMAN CHUAH ABDULLAH received the Ph.D. degree in chemical engineering from the University of Birmingham, U.K., in 2000. He is currently with the Institute for Tropical Forestry and Forest Products, Universiti Putra Malaysia. As an active researcher, he had published more than 300 journals and other publications. His research interests are in the areas of chemical processing, environmental engineering, oleochemical, air pollution control, energy storage and phase change materials, and process modelling and simulation. He also has a strong research collaboration with various national and international research institutions. He received the Young Engineer Award from the Institution of Engineers Malaysia (IEM), the Top Research Scientist Malaysia (TRSM) by the Academic of Science Malaysia, in 2013, and the Malaysia Rising Star Award by the Ministry of Higher Education, Malaysia, in 2015.